Photochemistry and Photobiology, 1997, 65(1): 107–114

Underwater Ultraviolet Radiation: Development of Spectral Models for Northern High Latitude Lakes

Isabelle Laurion*[1], Warwick F. Vincent[1] and David R. S. Lean[2]

[1]Département de biologie et Centre d'études nordiques, Université Laval, Sainte-Foy, Québec, Canada and [2]National Water Institute, Burlington, Ontario, Canada

Received 15 March 1996; accepted 23 September 1996

ABSTRACT

The penetration of solar ultraviolet radiation (UVR) and photosynthetically available radiation (PAR) was measured in a range of subarctic lakes in the forest–tundra zone of northern Québec. The diffuse attenuation coefficients for PAR (K_{dPAR}) were highly correlated (r^2 = 0.78) with dissolved organic carbon (DOC) concentration and only weakly correlated with suspended particulate material as measured by chlorophyll *a* (r^2 = 0.48) or beam transmittance (r^2 = 0.29). Colored dissolved organic matter (CDOM) was also largely responsible for the between-lake differences in spectral attenuation of UVR. The diffuse attenuation coefficient for UVR (K_d) was a nonlinear function of wavelength (λ) and was accurately described by the model K_d (λ) = K_{d440} exp(−S [λ-440]). The slope coefficient S was relatively constant among lakes (mean = 0.0151 nm^{-1}, CV = 7%), whereas K_{d440} was a linear function of several CDOM-related variables and best estimated by CDOM fluorescence (r^2 = 0.98). Numerical analysis of spectra for high (subarctic) and low (Arctic) DOC lakes showed that the evaluation of the model parameters K_{d440} and S was insensitive to the bandpass characteristics (2–8 nm) of different underwater radiometers. The K_d (λ) model was then used to develop a nondimensional index of relative spectral composition (RI) to characterize different water masses as a function of dissolved organic matter (DOC and CDOM fluorescence). Below about 4 mg DOC L^{-1} there is a sharp nonlinear rise in this index with decreasing DOC. These results show that CDOM controls the spectral composition of underwater UVR in northern high-latitude lakes and that the UVR/PAR balance in many of these waters is sensitive to minor changes in CDOM content.

INTRODUCTION

The photobiological effects of ultraviolet radiation (UVR)† in the aquatic environment are strongly determined by underwater spectral composition. Ultraviolet-B radiation (280–320 nm) is known to have a broad range of direct and indirect effects on aquatic biota (1), while UVA radiation (320–400 nm) and photosynthetically available radiation (PAR) have been implicated in repair as well as damage (2,3). The damaging effects of UV radiation are known to rise sharply with decreasing wavelength. For example, over the total UVR waveband (400 to 280 nm) the solar radiation flux drops by three orders of magnitude while the potential for DNA damage increases by three to five orders of magnitude (4). Net toxicity, however, is likely to reflect the wavelength-dependent balance between photochemical damage and biosynthetic repair (5).

Different UV wavelengths are attenuated to markedly different extents by natural waters, giving rise to major changes in UVR spectral composition with depth in marine and fresh waters (6). Most UV studies to date in the aquatic environment have used or calculated the attenuation of specific wavebands. For example, the diffuse attenuation coefficient for UVB (K_dB; integrated values between 300 and 320 nm) in temperate Canadian lakes can be described as a power function of dissolved organic carbon (DOC) and a linear function of the fluorescence of dissolved organic matter (7). Similar relations were found for UVA attenuation. Given the marked changes in spectral UVR with depth in combination with the strong nonlinearity in biological responses across the UVR waveband, more detailed information is required on the attenuation coefficients as a function of wavelength across the full solar UVR range.

Our objective in the present study was to develop models and indices that describe the spectral penetration of UVR into the lakes and rivers that compose a major element of the northern landscape. These high-latitude freshwater ecosystems are subject to rising UVB exposure associated with ozone depletion in the upper atmosphere (8). To achieve the widest application, underwater UVR models should ideally use relatively simple limnological descriptors rather than depend exclusively on expensive underwater UV profilers. Specifically, our aim was to define the vertical attenuation of solar irradiance as a function of wavelength for different biooptical conditions so that this information could then be combined with incident (modeled or measured) UVR data. We measured UVR attenuation in a range of optically contrasting lakes in subarctic Québec and in the Canadian high

*To whom correspondence should be addressed at: Département de Biologie, Université Laval, Sainte-Foy, Québec G1K 7P4, Canada. Fax: 418-656-2043; e-mail: COO1@music.ulaval.ca.

†*Abbreviations:* CDOM, colored dissolved organic matter; Chl *a*, chlorophyll *a*; DOC, dissolved organic carbon; PAR, photosynthetically available radiation; UVA, 320–400 nm radiation; UVB, 280–320 nm radiation; UVR, ultraviolet radiation.

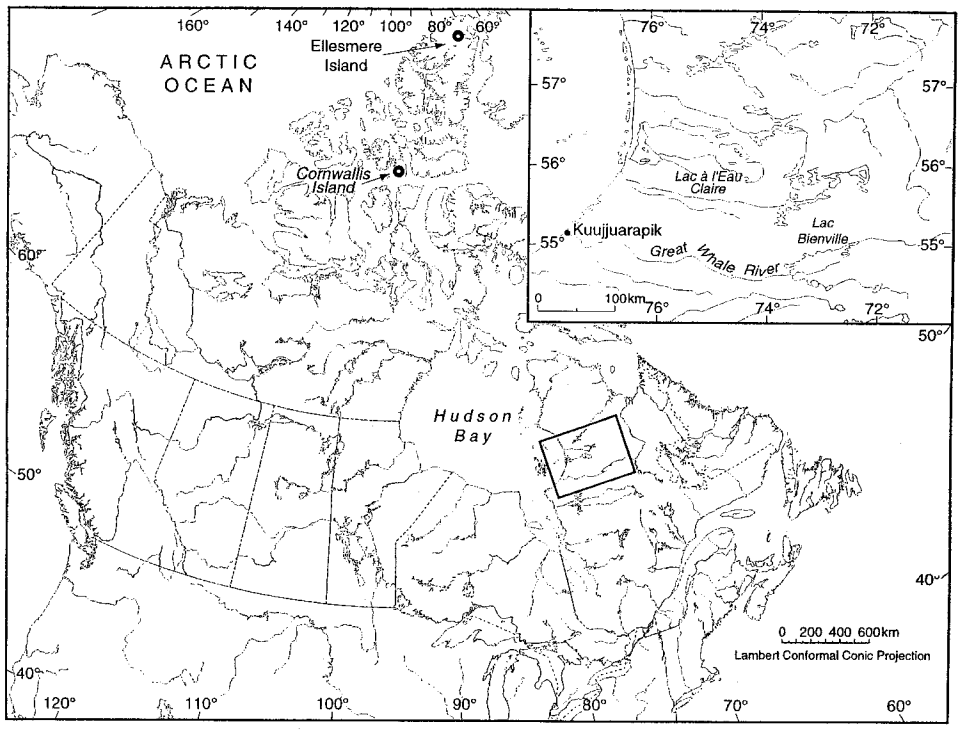

Figure 1. Location of the Arctic sampling sites (○) with three lakes near Resolute on Cornwallis Island and one on Ellesmere Island (Skeleton Lake) and of the subarctic sampling sites (insert).

Arctic. Using these profiles, we evaluated the influence of different light-absorbing components (phytoplankton as measured by chlorophyll *a* [Chl *a*]; colored or chromophoric dissolved organic matter [CDOM] measured in several ways) on downwelling solar radiation in the water column and the implications of bandpass of the underwater radiometer sensors for accurate estimates of UV spectral irradiance. This latter question is important because the various underwater UVR radiometers that are now commercially available differ in their bandpass characteristics (9). We then developed a general equation to describe UVR as a function of depth and wavelength and empirical methods to estimate the coefficients in this equation. We also obtained PAR profiles to further characterize the biooptical properties of these northern lakes. Finally, these relationships allowed us to develop an index of spectral composition in different water masses and to examine the implications of changing CDOM concentration on underwater UVR.

MATERIALS AND METHODS

Study sites. The first part of the study was conducted in the forest–tundra zone of subarctic Québec and included lakes and ponds in the vicinity of Kuujjuaraapik, Lac Bienville and Lac à l'Eau Claire, and the plume of the Great Whale River in Hudson Bay (Fig.1, insert). The waters within this transitional vegetation zone provided 18 stations with a wide range of CDOM concentrations. The second part of the study was conducted in the Arctic region (Fig. 1) in three lakes on Cornwallis Island close to Resolute (Meretta, Char and North) and one on Ellesmere Island (Skeleton). Sampling was during summer (July–August 1994) in both regions.

Optical measurements. The instrument used at the subarctic sites was a Biospherical PUV-500 radiometer that provides a measure of cosine-corrected downwelling irradiance at 305, 320, 340 and 380 nm (full bandwidth at half maximum is 8–10 nm) and of downwelling, cosine-corrected PAR (400–700 nm). This PUV was built in 1994 (serial number 9251) with the "new filter technology" (as described by Booth *et al.* (10)). A correction factor of 2.6 was applied to absolute irradiance at 305 nm as recommended in Kirk *et al.* (9). A Sea Tech beam transmissometer was connected to the profiler and gave the percentage of transmission of a collimated beam of 660 nm light across a 10 cm pathlength measuring cell (transmittance). The instrument also recorded depth and temperature. Profiles were generally taken within 3 h of solar noon.

The Arctic data were obtained with an Optronics OL 752 spectroradiometer. The instrument was set to take an irradiance measurement every 2 nm from 250 to 800 nm. The light sensor is a submersible PTFE-coated integrating sphere cosine receptor. This instrument obtains more detailed spectral data than the PUV-500 but is restricted to a maximum depth of measurement of 2.2 m. Two depths were used to evaluate K_d as a function of wavelength for the Optronics while the K_d values for the PUV-500 were determined from linear regressions of natural logarithm radiation against depth using all data points (10–100, depending on surface irradiance and wavelength) within the log-linear portion of the curve.

CDOM measurements. The CDOM characteristics at each site were determined by measurements of DOC concentration, CDOM fluorescence (F_{CDOM}) and CDOM absorption (a_{CDOM}). For these analyses the lake water was filtered through Sartorius 0.45 μm membrane filters immediately after collection and then stored in glass bottles (amber teflon-capped for the fluorescence samples) in the cold (4°C) and dark until analysis. The DOC was measured in these samples by high temperature oxidation with a Shimadzu TOC Analyzer model 5050 fitted with an ASI-5000 autosampler. The absorption coefficients (a_{CDOM}) were determined at 440 nm in a 1 cm cell with a Spectronic 1001plus spectrophotometer; these measurements were referenced against 0.22 μm membrane-filtered, double-distilled water.

The CDOM fluorescence was initially measured in a Shimadzu RF 5000U spectrofluorometer by emission scans from 360 to 600 nm with the excitation beam set to 348 nm and a slit width of 5 nm on both sides. For these measurements the fluorescence signal at 450 nm (peak height) was normalized to the Raman peak height. These measurements were subsequently repeated with a Perkin-Elmer LS50 spectrofluorometer to obtain an improved reference to the Raman signal as described by Determann *et al.* (11). The settings were as for the Shimadzu-5000 scans. All samples were measured in clean, fused silica cuvettes (SUPRASIL I) that were rinsed three times with the sample. Calibration of the instrument was done following Nieke *et al.* (12) and the CDOM fluorescence emission at

450 nm (peak height) was normalized to the Raman signal area to give F_{CDOM} in Raman units (nm^{-1}). These values were highly correlated with the peak height ratios obtained with the Shimadzu measurements ($r^2 = 0.93$).

Chlorophyll estimates. Samples for phytoplankton Chl *a* measurements were filtered onto MFS glass fiber filters (equivalent to GF/F filters) and then extracted in our field laboratory with boiling 90% (vol/vol) ethanol (13). The fluorescence of the extracts was measured with a Sequoia Turner model 450 fluorometer equipped with NB440 (blue excitation) and SC665 (red emission) filters.

Background theory and calculations. Bricaud *et al.* (14) have shown that the absorption coefficient (a) for natural filtered waters in the UV–visible region varies according to the relationship

$$a(\lambda) = a_0 \exp[-S(\lambda - \lambda_0)] \quad (1)$$

where S is a parameter describing the slope of the exponential curve and a_0 is the absorption coefficient at the reference wavelength λ_0. In a wide variety of Case 1 and Case 2 marine waters (*sensu* Jerlov (15)), as well as in many freshwater systems, S lies within the range of 0.010–0.023 nm^{-1} with a mean of 0.0156 nm^{-1} (12,14,16–19), while a_0 changes greatly with the concentration of CDOM. This colored portion of DOM, specifically that associated with the humic and fulvic acid fractions, appears to control this characteristic absorbance curve (14) as well as the fluorescence emission properties of filtered natural waters (11).

We hypothesized that the diffuse attenuation coefficient (K_d) would follow the same exponential function of wavelength in the UV spectral region as for Eq. 1:

$$K_d(\lambda) = K_{d440} \exp[-S(\lambda - 440)] \quad (2)$$

where S would be a constant and where K_{d440}, the attenuation coefficient at a reference wavelength of 440 nm, would be a function of CDOM variables. It should be noted that unlike 'a', which is an inherent optical property, K_d is an apparent optical parameter, because it is dependent on the angular distribution of the irradiance in addition to the dissolved and suspended materials in the water (20).

The $K_d(\lambda)$ values were obtained from the depth profiles of solar radiation as above. These values were fitted by least-squares regression to Eq. 2 that gave estimates of S and K_{d440} for each station. Correlation analysis was then used to determine the relationship between K_{d440} and the measured parameters DOC, F_{CDOM}, a_{CDOM} at 440 nm (a_{440}), transmittance and Chl *a*.

RESULTS

Underwater PAR

The study sites encompassed a broad range of transparencies in the PAR waveband with diffuse attenuation coefficient values ranging from 0.19 to 1.52 m^{-1}. Unlike clear oceanic waters (20), there was minimal change in the slope of log PAR irradiance *versus* depth, and attenuation was well characterized by a single K_{dPAR} for each site. These values were highly correlated ($r > +0.88$, $P < 0.001$) with the variables associated with CDOM, *i.e.* DOC, F_{CDOM} and a_{440} (Fig. 2). The best predictor was a_{440} which explained 83% of the variance in K_{dPAR}. The K_{dPAR} was more weakly correlated with Chl *a* concentration ($r = +0.69$, $P < 0.002$, Fig. 2D) and transmittance ($r = -0.54$, $P < 0.05$).

Influence of surface conditions

Local meteorological conditions at the time of measurement influenced the variability in underwater irradiance as seen by the dispersion of points around the regression for obtaining K_d (Fig. 3). Under sunny, clear sky conditions with low-amplitude surface waves (<8 cm), the PAR values were scattered widely around the regression curve (Fig. 3A). This variability was not observed under flat calm conditions (Fig. 3C) nor under overcast skies, even when there was considerable surface wave activity (30–40 cm, Fig. 3E).

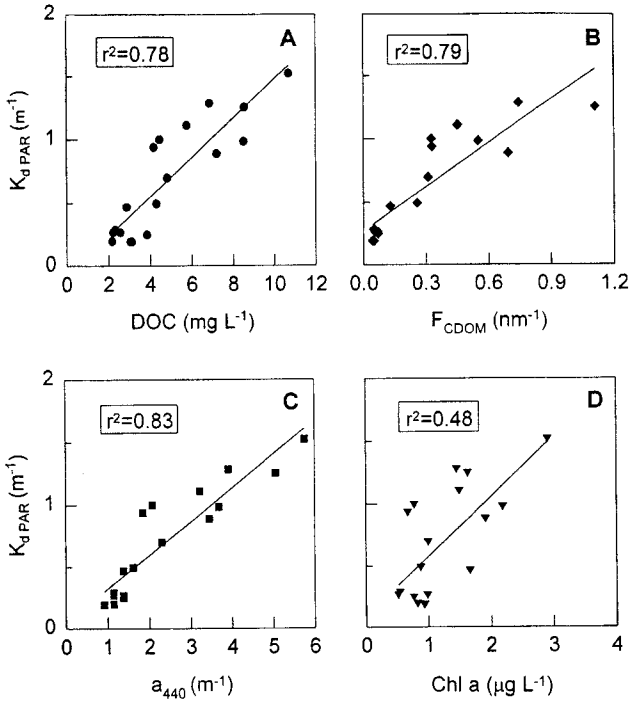

Figure 2. Relationship between the diffuse attenuation coefficient for PAR (K_{dPAR}) and different limnological parameters: DOC (A), CDOM fluorescence (B), absorption coefficient at 440 nm (C) and chlorophyll *a* concentration (D). For all regression analyses, $P < 0.005$.

The variability under clear skies was strongly dependent on wavelength. There was a decreasing dispersion of points around the regression curves with decreasing wavelength across the UVR range (Fig. 3B). These observations underscore the influence that local meteorological conditions can have on the variability in underwater spectral balance experienced by planktonic organisms in the surface mixed layer. For example, under the clear sky and surface wave conditions in Fig. 3, PAR fluxes at 30 cm varied by approximatively ±20%, while the UVR at 320 nm at this depth varied by ±5%.

Application of the $K_d(\lambda)$ function

For all 18 profiles obtained in the subarctic, there was a good fit between measured K_d values and the exponential $K_d(\lambda)$ model given in Eq. 2. S varied little (mean = 0.0151 nm^{-1}, CV = 7%; Table 1) and was within the range for literature values derived from absorption spectra. For these analyses, the 305 nm channel was generally not included for two reasons. First, there was a large variance in K_d at this wavelength between repeated profiles that may in part be due to inadequate depth resolution by the pressure sensor. Second, the log-linear regressions with the data at this wavelength often gave estimates of K_d that deviated subtantially from the close fit of the 320, 340 and 380 nm data to the $K_d(\lambda)$ function. In 5 out of the 18 stations, the measured K_{d305} was below the measured K_{d320} (see Table 1). Correction of these measurements by field readings of the instrument dark offset

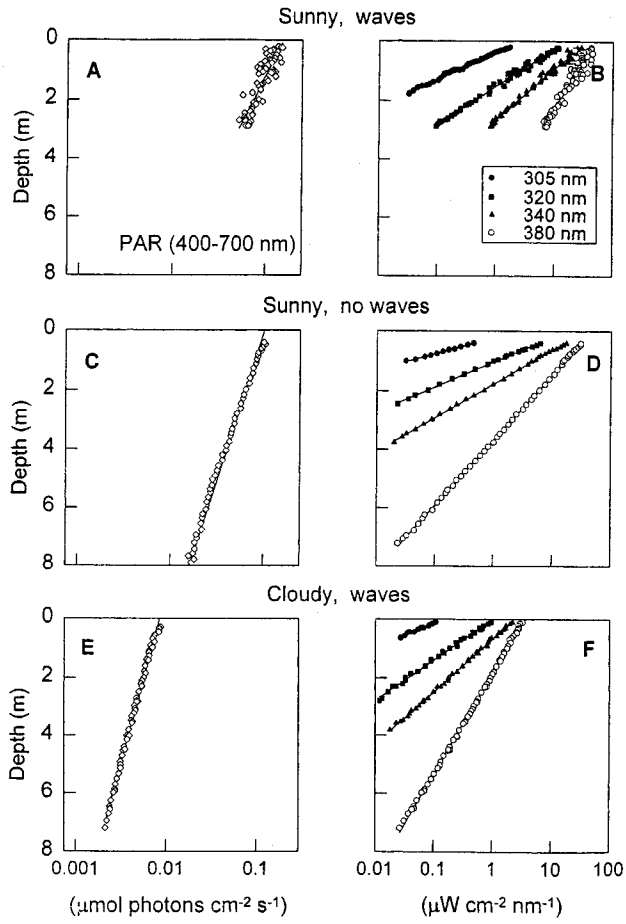

Figure 3. Influence of meteorological conditions on the variability in underwater PAR (A, C and E) and UVR (B, D and F) at Lac à l'Eau Claire.

Table 1. The DOC, K_d at 305, 320, 340 and 380 nm and slope coefficients for the K_d (λ) function for subarctic and Arctic sites*

Station	DOC (mg L^{-1})	K_{d305} (m^{-1})	K_{d320} (m^{-1})	K_{d340} (m^{-1})	K_{d380} (m^{-1})	S (nm^{-1})
Kuujjuaraapik region						
K1	4.82	*10.84*	11.55	8.74	4.44	0.0161
K2	7.22	*23.33*	22.41	17.37	9.76	0.0139
K3	8.56	43.17	25.77	24.06	13.78	0.0138
K4	5.77	26.37	20.07	14.69	8.38	0.0151
Great Whale River plume						
K6	4.46	*11.37*	10.96	8.81	5.08	0.0130
K7	4.18	*10.88*	11.08	8.85	4.98	0.0135
Lac Bienville						
B1	4.31	*8.51*	9.83	7.06	3.76	0.0160
Lac à l'Eau Claire						
C1	8.52	*12.68*	18.92	15.02	7.87	0.0148
C2	6.87	*7.63*	23.13	17.45	9.68	0.0145
C3	2.33	*2.57*	1.79	1.33	0.67	0.0165
C4	2.18	2.32	1.92	1.35	0.69	0.0164
C5	2.87	*5.06*	5.01	3.94	2.09	0.0148
C6	2.57	*4.33*	3.11	2.28	1.23	0.0155
C7	3.85	*3.59*	2.68	2.05	1.06	0.0156
C8	2.23	*3.04*	2.11	1.58	0.86	0.0150
C9	3.06	*2.53*	1.85	1.37	0.71	0.0160
C10	10.71	na	40.80	27.55	16.15	0.0151
C11	3.10	*2.72*	1.67	1.28	0.67	0.0154
Mean						0.0151
Standard deviation						0.0010
Arctic lakes						
Char	0.90	0.92	0.75	0.60	0.44	0.0135
North	1.10	1.41	1.03	0.69	0.41	0.0186
Meretta	2.30	2.25	1.75	1.28	0.86	0.0152
Skeleton	5.40	9.44	7.89	5.71	2.77	0.0170

*When DOC was too high, K_{d305} was not available (na). The K_{d305} given in italics were not used for obtaining the regression of K_d (λ).

(*i.e.* with an opaque neoprene cap over the sensor) produced only minor changes (*ca* 6%) in the K_{d305} estimates and could not account for the deviations.

The relationship between the diffuse attenuation coefficient for downwelling irradiance and wavelength for the surface waters of the four Arctic lakes was also examined. S was more variable than in the subarctic (mean = 0.0161 nm^{-1}, CV = 13.7%) with highest values that were near the upper limit of the literature range for absorption spectra (Table 1). Most of the Arctic spectra were obtained in windy conditions or under partial cloud cover, which could decrease the precision in the evaluation of K_d and thus of S.

The K_{d440} showed a strong and positive correlation ($r > +0.95$, $P < 0.001$) with CDOM variables: DOC (Fig. 4A), F_{CDOM} (Fig. 4B) and a_{440} (Fig. 4C). There was a weaker correlation with Chl *a* ($r = +0.79$, $P < 0.001$; Fig. 4D) and with transmittance ($r = -0.40$, $P > 0.1$). The latter correlation improved when the turbid stations of the Great Whale River plume were removed ($r = -0.72$, $P < 0.01$).

Effect of bandpass

Numerical analyses of high-resolution spectral data simulated for a lake containing 8 mg DOC L^{-1} (generated with the subarctic regression equation for K_{d440} as a function of DOC, a representative incident spectrum and the Eq. 2 for K_d [λ]) showed that a moderate increase in bandpass of the UV sensors should not seriously compromise the evaluation of spectral irradiance. For this calculation we integrated irradiance values over 4 nm, 8 nm (the full bandwidth at half maximum of the PUV-500 radiometer sensors is 8–10 nm), 16 nm and 24 nm, considering a flat response across each selected waveband. These values were used to recalculate K_d as a function of wavelength and to determine S and K_{d440} relative to those obtained using the original UVR values at 2 nm resolution (Table 2). The wavelength range over which the bandpass simulation analysis was conducted was 280 to 400 nm. For the integration with an 8 nm bandpass, S was 1% below the estimates with a 2 nm bandpass and K_{d440} increased by 1%. We obtained almost identical results for the same calculations based on a lake with 3 mg DOC L^{-1} (<5% variation in S and K_{440} for bandpasses from 2 to 16 nm). We then repeated these calculations using a set of field data obtained at 2 nm resolution from Char Lake (from 300 to 355 nm), a low DOC lake in the high Arctic. The 4 nm and 8 nm integrations gave little change (1–4%) relative to the original 2 nm data, however more substantial changes occurred for simulated bandpasses of 16 and 24 nm (Table 2).

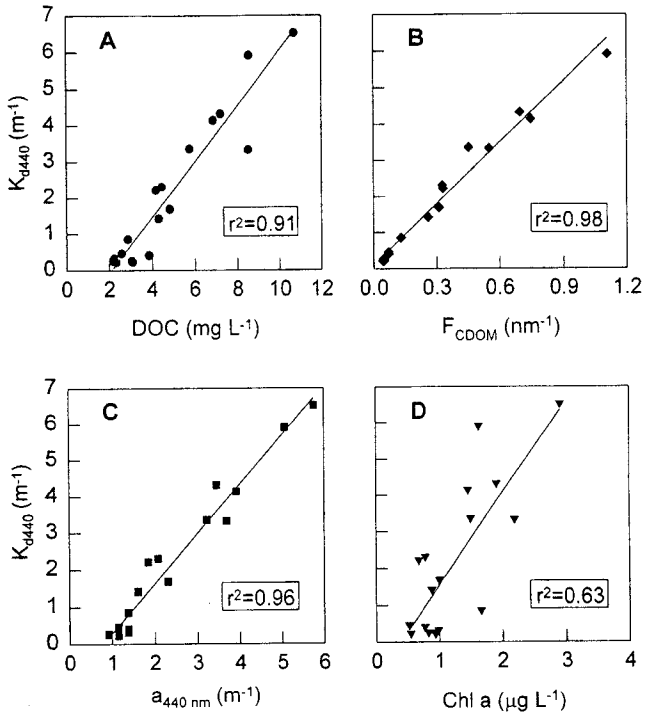

Figure 4. Relationship between the diffuse attenuation coefficient at the reference wavelength 440 nm (K_{d440}) and different limnological parameters: DOC concentration (A), CDOM fluorescence (B), absorption coefficient at 440 nm (C) and Chl *a* concentration (D). For all regression analyses, $P < 0.001$.

DISCUSSION

Our data for high-latitude lakes from northern Canada show that CDOM has a major influence on underwater PAR attenuation and explains a large percentage (*ca* 80%) of the optical variability between lakes. This conclusion is consistent with observations from further south on the Canadian Shield where DOC, not phytoplankton, has been identified as a primary control on attenuation of visible light in Experimental Lake Area lakes (21). Similarly, in a south–north transect of lakes from the boreal forest to the Arctic tundra, Pienitz *et al.* (22) found a strong inverse correlation between Secchi disk transparency and DOC.

The present study shows that spectral irradiance across the UVR range in northern lakes is tightly controlled by CDOM. The equation $K_d(\lambda) = K_{d440} \exp(-S[\lambda - 440])$ provides an accurate description of the attenuation of underwater downwelling UV irradiance, and the intercept K_{d440} is strongly correlated with CDOM-related variables (DOC, F_{CDOM} and a_{440}). The slope S varied little among lakes (CV = 7%) and was similar to literature values for absorbance curves for filtered natural waters. This remarkable constancy of S can also be seen from the data presented by Scully and Lean (7), the first compilation of K_d values for UVR attenuation in a wide range of North American lakes (lat. 41–51°N). Our Eq. 2 model gave an excellent fit ($r^2 > 0.94$) to their tabulated K_d values for 300, 310, 320, 340 and 380 nm, with a mean S of 0.0150 nm^{-1} and a coefficient of variation of 17%. More recently, Morris *et al.* (23) found a mean slope of 0.0135 nm^{-1} (n = 59, CV = 4%) for a wide range of lakes extending from Alaska to Argentina, including many low DOC lakes (<1 mg DOC L^{-1}).

Table 2. Slopes and intercepts of the $K_d(\lambda)$ function calculated for different sensor bandpasses*

Sensor bandpass (nm)	S (nm^{-1})		K_{d440} (m^{-1})	
	Simulated (high DOC)	Field (low DOC)	Simulated (high DOC)	Field (low DOC)
2	0.0151	0.0135	0.1569	0.1569
4	0.0151 (<1)	0.0133 (1)	0.1591 (<1)	0.1591 (1)
8	0.0149 (1)	0.0131 (3)	0.1635 (1)	0.1635 (4)
16	0.0144 (5)	0.0112 (17)	0.1951 (4)	0.1951 (24)
24	0.0137 (9)	0.0095 (30)	0.2350 (6)	0.2350 (50)

*Deviations (%) from the 2 nm-based estimates are given in parentheses. The simulated values at 2 nm resolution were generated using Eq. 2, S = 0.0151 nm^{-1} and K_{d440} estimated for 8 mg DOC L^{-1} from the regression given in Fig. 4A. The field values were obtained from measurements in Char Lake (0.9 mg DOC L^{-1}) with the Optronics scanning radiometer using a bandpass of 2 nm.

For the estimates of S for the subarctic lakes, we generally excluded data from the 305 nm channel of the PUV-500. The high variability in K_d between repeated profiles with this channel reflects the low solar UVR flux at this wavelength and its rapid attenuation to values approaching the noise level of the instrument. A more sensitive pressure-depth sensor on this instrument (as in the PUV-501) would have improved our ability to profile shallow lakes and DOC-rich waters. Many of the subarctic 305 nm profiles gave a good log-linear fit ($r^2 > 0.94$), but the resultant K_d values deviated substantially from the $K_d(\lambda)$ trend observed with the three other UVR channels. This effect was never observed in the spectral absorbance scans of filtered water. We are unable to determine at this stage whether this represents a design limitation of the 305 nm channel of the PUV-500, or whether it is a real effect on the apparent property K_{d305} caused by specific lighting conditions. This effect has not been previously noted using narrow waveband spectroradiometers in a wide range of temperate lakes (7) nor in our Arctic lake measurements with the Optronics (OL 752). However, we find a similar effect in Table 1 of Morris *et al.* (23), who also used a PUV instrument.

Although most of the values of S reported here and in the literature fall within the same narrow range, there are some notable exceptions that could be related to DOM chemical composition. Howard-Williams and Vincent (16) have shown in a study of 34 New Zealand lakes, ranging from oligotrophic alpine lakes to low-altitude humic-stained lakes, that S for absorbance spectra was constant except for geothermal lakes that contain dense microalgal and/or bacterial concentrations. For these lakes, S was higher. Vincent and Forsyth (24) hypothesized that this difference could be due to the presence of autochthonous DOM that may be of a nonhumic nature. Certain amino acids, for example, absorb in the UVB and UVC wavebands and can be quantitated by fluorescence spectroscopy (11). The absorbance data reported for Antarctic lakes (characterized by extremely low allochthonous inputs; (25)) also give higher S values. For the four Arctic lakes in our study, the mean slope was slightly

higher than for the subarctic stations and may similarly reflect low inputs of allochthonous DOM from the sparsely vegetated catchments of the high Arctic region. Green and Blough (26) found for the Florida coast and the Gulf of Mexico a wider range of S values for absorption spectra (from 0.014 to >0.030 nm^{-1}). Their lowest values of S corresponded to inland and coastal samples, while the offshore blue waters generally exhibited higher values of S, again suggesting a shift away from allochthonous dominance of the DOM pool. Thus, before estimating spectral UV irradiance from CDOM measurements, the possibility of unusual S values should be evaluated by absorbance scans of filtered water from the particular region of interest. It may not be advisable, however, to directly apply S derived from a (λ) as an estimate of K_d (λ) because there is some evidence that these two slopes can deviate (23). In future research on underwater UVR it would be useful to determine the magnitude of this discrepancy for different ranges of DOC concentration and determine to what extent it varies with different instruments and measurement protocols.

The goodness-of-fit of the K_d (λ) model indicates that it can be applied with confidence to northern lakes and rivers by using a mean value of S of 0.015 nm^{-1} and by estimating K_{d440} from one of the CDOM variables. The common use of a_{440} as a limnological index of water color (6), combined with its ease of measurement, makes this variable particularly attractive for estimation of K_{d440}. Such an approach would also allow estimates of UVR penetration based on historical records. Several precautions, however, should be considered. The present study examined lakes with a range 0.5–3 μg Chl *a* L^{-1} and the relationships obtained here may not apply outside this range, *i.e.* to phytoplankton-rich waters. Our K_d (λ) function also assumes an optically homogeneous water mass; changes in UV-absorbing components down the water column, for example by bleaching of DOM in the surface waters, will also lessen the accuracy of this model. Finally, the use of DOC measurements to estimate K_{d440} in the K_d (λ) function is limited to lakes that have DOC concentrations greater than 2 mg L^{-1} (the lower limit of our subarctic data range), below which DOC may be of a different nature and may have a lower colored fraction (7,27). The use of F_{CDOM} or a_{CDOM}, which are direct properties of the colored fraction of DOM, may overcome this problem.

Our calculations using high spectral resolution UVR values show that there is little bias created by using sensors with a moderately wide bandpass (*ca* 10 nm) at either high or low DOC concentrations. The exponential drop in K_d with wavelength means that the signal output from broad bandpass sensors will be biased toward longer wavelengths and to an increasing extent with depth (9). Large bandpass sensors therefore underestimate true K_d, to the greatest extent within the UVB range. These effects, however, appear to be negligible up to at least 8 nm, which is close to the bandpass of the PUV-500.

Spectral irradiance across the UVR and PAR range appears to influence strongly the balance between biological damage and repair in planktonic communities (5). It is therefore important to examine how the relationships found in the present study can be used to quantify spectral balance for comparisons between depths and between different lakewaters. At any depth z, the ratio of UVR at a specified wavelength (E_{UVW}) to PAR (E_{PAR}) is given by

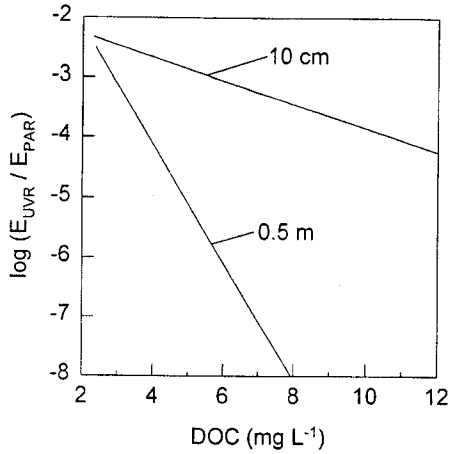

Figure 5. The ratio of UVW to PAR at two arbitrary depths as a function of DOC. The curves were obtained by using the linear regression models from the present study and a continuous set of DOC values (Fig. 2 and 4 for K_{dPAR} and K_{d440} and Eq. 2 with an S of 0.0151 nm^{-1} for K_{dUVW}).

$$E_{UVW}/E_{PAR} = R_{atm} \exp(-\Delta K z) \quad (3)$$

where R_{atm} is the incident irradiance ratio just beneath the water surface (E_{0UVW}/E_{0PAR}) and is dependent on weather conditions, solar zenith angle, altitude and atmospheric ozone concentration (2,28), and ΔK is the difference between the UVW and PAR diffuse attenuation coefficients. Because of the strong CDOM influence on K_{dUVW} and K_{dPAR}, ΔK is also a close linear function of CDOM variables. For these calculations we used the 320 nm irradiance data because it is at the boundary of UVB and UVA. For comparisons between lakes at two specified depths and for a constant R_{atm}, E_{UVW}/E_{PAR} is a negative exponential function of CDOM, here represented by the most common descriptor of DOC (Fig. 5). The modeled relations were obtained by using regressions on Figs. 2 and 4 to get K_{dPAR} and K_{d440}, Eq. 2 with an S of 0.0151 nm^{-1} to estimate K_{dUVW} (at 320 nm) and a representative R_{atm} of 0.005. These curves show the strong nonlinear influence of CDOM on spectral composition as a function of depth. For aquatic systems where K_{dPAR} varies substantially with depth (*e.g.* ultraoligotrophic oceans), K_d could be estimated at a specified wavelength in the visible range of the spectrum (*e.g.* 440 nm), instead of the entire PAR waveband, to characterize the UVR/PAR spectral balance.

An alternative way of comparing spectral balance between lakes is to compute the ratio of water column integrals for E_{UVW} and E_{PAR} (RI), each integrated from the surface down to the depth z_x at which the radiation is reduced to a fixed percentage x of surface values (*e.g.* x = 1% E_o)

$$RI = \int E_{UVW}\, dz / \int E_{PAR}\, dz. \quad (4)$$

This ratio of integral exposure is of particular relevance to plankton communities circulating through the surface mixed layer (epilimnion or diurnal mixed layer). The water column integral for E_{UVW} is given by

$$\int E_{UVW}\, dz = \int E_{oUVW} \exp(-K_{dUVW} z)\, dz. \quad (5)$$

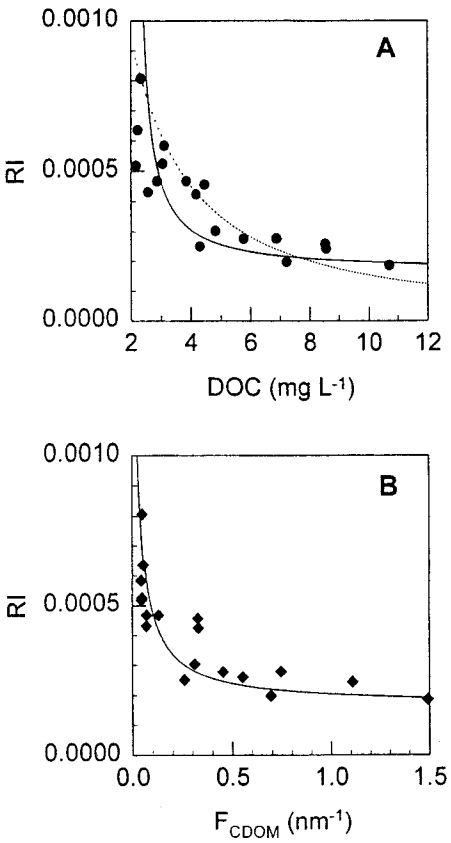

Figure 6. Relationship between RI and DOC (A) or F_{CDOM} (B). Solid lines were obtained by using models from the present study and a continuous set of DOC and F_{CDOM} values (Figs. 2 and 4 to get K_{dPAR} and K_{d440} and Eq. 2 with a S of 0.0151 nm^{-1} to get K_{dUVW}). The dotted line was obtained by applying the nonlinear model for K_{d440} as a function of DOC (as suggested by Scully and Lean (7)) to our data ($r^2 = 0.85$, $P < 0.001$) instead of using the linear regression from Fig. 4. Individual points are from the field measurements in the subarctic.

Evaluating this integral from the surface (z = 0) to the depth of x% of E_{oUVW} ($z = z_{xUVR}$) gives

$$\int E_{UVW}\, dz = E_{oUVW}\,[\exp(-K_{dUVW}z_{xUVW}) - 1]/K_{dUVW}. \quad (6)$$

Deriving the same expression for $\int E_{PAR}\, dz$ (as used for example in the Riley expression of average water column irradiance (29)), substituting in Eq. 4 and simplifying the expression gives

$$RI = R_{atm}(K_{dPAR}/K_{dUVW}). \quad (7)$$

The ratio K_{dPAR}/K_{dUVW} is a dimensionless index (like RI) and is algebraically equivalent to the ratio z_{xUVW}/z_{xPAR} (for any value of x).

In Fig. 6 we calculated the RI index for each of our subarctic profiling sites and plotted these values against DOC and F_{CDOM}. For these calculations we used the 320 nm irradiance data as above. We used a mean R_{atm} of 0.005 and considered it to be constant for our 18 stations. The RI index was calculated from the UVW and PAR profiles (giving individual data points) and from the linear regression relationships for K_{dPAR} and K_{dUVW} to generate continuous functions (solid lines; *e.g.* for DOC = 10 mg L^{-1}, $K_{dPAR} = 0.154[10] - 0.068$; $K_{d440} = 0.767[10] - 1.606$; S = 0.0151 nm^{-1}; $K_{dUVW} = K_{d440}\exp[-S(320–440)]$; RI = 1.98×10^{-4}). In Fig. 6A, the same calculation was repeated using a power function to obtain K_{d440} (dashed line; $K_{d440} = 0.044[DOC]^{2.25}$, $r^2 = 0.85$) as suggested by Scully and Lean (7) and discussed in McKnight *et al.* (27). The resultant plots show the strong nonlinear relationship between proportional UVW penetration and CDOM variables. There is very little change over the range 4–11 mg DOC L^{-1} (or 0.2–1.5 Raman units) but at DOC concentrations less than 4 mg L^{-1} there is a marked nonlinear upswing in relative UVW, indicating a high sensitivity to small changes in CDOM. The scatter of the data points about the lines is at least partly the result of variations in incident R_{atm}.

For the case where the surface mixed layer is shallower than the euphotic zone, this index does not represent the optical conditions that near-surface phytoplankton experience. For this situation, the irradiances should be summed to the depth limit of mixing (z_m instead of z_x) and Eq. 4 can be solved as

$$RI = R_{atm}(K_{dPAR}/K_{dUVW}) \cdot [\exp(-K_{dUVW}z_m) - 1]/[\exp(-K_{dPAR}z_m) - 1] \quad (8)$$

Lakes on the Canadian Shield appear to be becoming clearer as a result of reduced concentrations of DOM; this effect has been attributed to the changing water balance of the lakes and catchments as a result of global warming (21). Other perturbations such as acidification and bleaching due to increased UVB can also lead to a DOC decline in lakes (30,31). For the many northern lakes that have DOM concentrations at or below 4 mg DOC L^{-1} (*e.g.* for lakes on a transect from Yellowknife to Contwoyto Lake, North West Territories, mean DOC is 4.3 mg L^{-1} (22)) a small decrease in DOM would lead to major changes in the biologically important UVR/PAR spectral balance. These northern freshwater ecosystems may therefore be especially sensitive to the biooptical effects of global change.

Acknowledgements—The authors thank Sylvain Arsenault and Mylène Bergeron for their assistance in the field, Barbara Nieke, Norm Scully and Craig Williamson for providing valuable comments at various stages in this research, Barbara Nieke for kindly running the Perkin-Elmer F_{CDOM} analyses and Martin Poitras for drafting Fig. 1. The comments of P. J. Neale and an anonymous referee during the review process were greatly appreciated. This research was funded by the Centre d'études nordiques (Université Laval), the Ministry of Northern & Indian Affairs and NSERC. Logistic support in the Arctic was provided by the Polar Continental Shelf Project (Canada). This is publication number PCSP/ÉPCP/26.

REFERENCES

1. Williamson C. E. and H. E. Zagarese (1994) Impact of UV-B radiation on pelagic freshwater ecosystems. *Arch. Hydrobiol. Beih. Ergebn. Limnol.* **43**, 1–226.
2. Karentz, D., J. E. Cleaver and D. I. Mitchell (1991) Cell survival characteristics and molecular responses of Antarctic phytoplankton to ultraviolet-B radiation. *J. Phycol.* **27**, 326–341.
3. Quesada, A., J.-L. Mouget and W. F. Vincent (1995) Growth of Antarctic cyanobacteria under ultraviolet radiation: UVA counteracts UVB inhibition. *J. Phycol.* **31**, 242–248.
4. Vincent, W. F. and S. Roy (1993) Solar UV-B and aquatic primary production: damage, protection and recovery. *Environ. Rev.* **1**, 1–12.
5. Smith, R. C., B. B. Prezélin, K. S. Baker, R. R. Bidigare, N. P.

Boucher, T. Coley, D. Karentz, S. MacIntyre, H. A. Matlick, D. Menzies, M. Ondrusek, Z. Wan and K. J. Waters (1992) Ozone depletion: ultraviolet radiation and phytoplankton biology in Antarctic waters. *Science* **255**, 952–959.
6. Kirk, J. T. O. (1994) *Light and Photosynthesis in Aquatic Ecosystems.* Cambridge University Press, Cambridge.
7. Scully, N. M. and D. R. S. Lean (1994) The attenuation of ultraviolet radiation in temperate lakes. *Arch. Hydrobiol. Beih. Ergebn. Limnol.* **43**, 135–144.
8. International Arctic Science Committee (1995) Effects of increased ultraviolet radiation in the Arctic. IASC Report No. 2, Oslo, Norway, 56 p.
9. Kirk, J. T. O., B. R. Hargreaves, D. P. Morris, R. B. Coffin, B. David, D. Frederickson, D. Karentz, D. R. S. Lean, M. P. Lesser, S. Madronich, J. H. Morrow, N. B. Nelson and N. M. Scully (1994) Measurements of UV-B radiation in two freshwater lakes: an instrument intercomparison. *Arch. Hydrobiol. Beih. Ergebn. Limnol.* **43**, 71–99.
10. Booth, C. R., T. Mestechkina and J. H. Morrow (1994) Errors in the reporting of solar spectral irradiance using moderate bandwidth radiometers: an experimental investigation. *Ocean Optics XII* **2258**, 654–663.
11. Determann, S., R. Reuter, P. Wagner and R. Willkomn (1994) Fluorescent matter in the eastern Atlantic Ocean part 1: method of measurement and near-surface distribution. *Deep-Sea Res.* **41**, 659–675.
12. Nieke, B., R. Reuter, R. Heuermann, H. Wang, M. Babin and J.-C. Therriault (1996) Light absorption and fluorescence properties of chromophoric dissolved organic matter (CDOM), in the St. Lawrence Estuary (case 2 waters). *Cont. Shelf Res.* (In press).
13. Nusch, E. A. (1980) Comparison of different methods for chlorophyll and phaeopigment determination. *Arch. Hydrobiol. Beih. Ergebn. Limnol.* **14**, 14–36.
14. Bricaud, A., A. Morel and L. Prieur (1981) Absorption by dissolved organic matter of the sea (yellow substance) in the UV and visible domains. *Limnol. Oceanogr.* **26**, 43–53.
15. Jerlov, N. G. (1976) *Marine Optics.* Amsterdam, Elsevier.
16. Howard-Williams, C. and W. F. Vincent (1985) Optical properties of New Zealand lakes: II. Underwater spectral characteristics and effects on PAR attenuation. *Arch. Hydrobiol.* **104**, 441–457.
17. Davies-Colley, R. J. and W. N. Vant (1987) Absorption of light by yellow substance in freshwater lakes. *Limnol. Oceanogr.* **32**, 416–425.
18. Diebel, D. (1987) Tiefenaufgelöste Laserfernerkundung geschichteter Strukturen im Meer unter Verwendung von Gelbstoff als Tracersubstanz. PhD thesis, University of Oldenburg, Germany.
19. Hoge, F. E., A. Vodacek and N. V. Blough (1993) Inherent optical properties of the ocean: retrieval of the absorption coefficient of chromophoric dissolved organic matter from fluorescence measurements. *Limnol. Oceanogr.* **38**, 1394–1402.
20. Smith, R. C. and K. S. Baker (1981) Optical properties of the clearest natural waters (200–800 nm). *Appl. Opt.* **20**, 177–184.
21. Schindler, D. W., K. G. Beaty, E. J. Fee, D. R. Cruikshank, E. R. Debruyn, D. L. Findlay, G. A. Linsey, J. A. Shearer, M. P. Stainton and M. A. Turner (1990) Effects of climatic warming on lakes of the central boreal forest. *Science* **250**, 967–970.
22. Pienitz, R., J. P. Smol and D. R. S. Lean (1996) Physical and chemical limnology of 24 lakes located between Yellowknife and Contwoyto Lake, Northwest Territories (Canada). *Can. J. Fish. Aquat. Sci.* (In press).
23. Morris, D. P., H. Zagarese, C. E. Williamson, E. G. Balseiro, B. R. Hargreaves, B. Modenutti and C. Queimalinos (1995) The attenuation of solar UV radiation in lakes and the role of dissolved organic carbon. *Limnol. Oceanogr.* **40**, 1381–1391.
24. Vincent, W. F. and D. J. Forsyth (1987) Geothermally influenced waters. In *Inland Waters of New Zealand* (Edited by A. B. Viner), pp. 349–377. DSIR Science Information Publishing Center, Wellington, New Zealand.
25. McKnight, D. M., E. D. Andrews, S. A. Spaulding and G. R. Aiken (1994) Aquatic fulvic acids in algal-rich antarctic ponds. *Limnol. Oceanogr.* **39**, 1972–1979.
26. Green, S. A. and N. V. Blough (1994) Optical absorption and fluorescence properties of chromophoric dissolved organic matter in natural waters. *Limnol. Oceanogr.* **39**, 1903–1916.
27. McKnight, D. M., R. Harnish, R. L. Wershaw, J. S. Baron and S. Schiff (1996) Chemical characteristics of particulate, colloidal, and dissolved organic material in Loch Vale watershed, Rocky Mountain National Park. *Biogeochemistry.* (In press)
28. Arrigo, K. R. (1994) Impact of ozone depletion on phytoplankton growth in the Southern Ocean: large-scale spacial and temporal variability. *Mar. Ecol. Prog. Ser.* **114**, 1–12.
29. Riley, G. A. (1957) Phytoplankton of the North Central Sargasso Sea. *Limnol. Oceanogr.* **2**, 252–270.
30. Schindler, D. W., P. J. Curtis, B. R. Parker and M. P. Stainton (1996) Consequence of climate warming and lake acidification for UV-B penetration in North American boreal lakes. *Nature* **379**, 705–708.
31. Yan, N. D., W. Keller, N. M. Scully, D. R. S. Lean and P. J. Dillon (1996) Increased UV-B penetration in lake owing to drought-induced acidification. *Nature* **381**, 141–143.

Erratum

Laurion I, Vincent WF, Lean DRS 1997. Underwater ultraviolet radiation: development of spectral models for northern latitude lakes. Photochem. Photobiol. 65: 107-114.

Table 2. Slopes and intercepts of the K_d (λ) function calculated for different sensor bandpasses*

Sensor band-pass (nm)	S (nm^{-1})		K_{d440} (m^{-1})	
	Simulated (high DOC)	Field (low DOC)	Simulated (high DOC)	Field (low DOC)
2	0.0151	0.0135	**4.530**	0.1569
4	0.0151 (<1)	0.0133 (1)	**4.5398 (<1)**	0.1591 (1)
8	0.0149 (1)	0.0131 (3)	**4.5703 (1)**	0.1635 (4)
16	0.0144 (5)	0.0112 (17)	**4.6945 (4)**	0.1951 (24)
24	0.0137 (9)	0.0095 (30)	**4.8208 (6)**	0.2350 (50)

* Deviations (%) from the 2 nm-based estimates are given in parentheses. The simulated values at 2 nm resolution were generated using Eq. 2.2, S = 0.0151 nm^{-1} and K_{d440} estimated for 8 mg DOC L^{-1} from the regression given in Fig. 4A. The field values were obtained from measurements in Char Lake (0.9 mg DOC L^{-1}) with the Optronics scanning radiometer using a bandpass of 2 nm.